Superfluid ^{4}He Quantum Interference Grating

Yuki Sato, Aditya Joshi, and Richard Packard

Physics Department, University of California, Berkeley, California 94720, USA

(Received 27 May 2008; revised manuscript received 8 July 2008; published 22 August 2008)

We report the first observation of quantum interference from a grating structure consisting of four weak link junctions in superfluid ^{4}He. We find that an interference grating can be implemented successfully in a superfluid matter wave interferometer to enhance its sensitivity while trading away some of its dynamic range. We also show that this type of device can be used to measure absolute quantum mechanical phase differences. The results demonstrate the robust nature of superfluid phase coherence arising from quantum mechanics on a macroscopic scale.

DOI: 10.1103/PhysRevLett.101.085302 PACS numbers: 67.25.dg, 03.75.−b, 85.25.Dq

Detectors based on superconducting quantum interference are the essential ingredient for many scientific endeavors [1]. The most widely used device is the dc SQUID, which utilizes two Josephson junctions placed in a superconducting loop. The sensitivity of these interferometers can be increased even further by placing more than two junctions in parallel thus narrowing the peaks in the interference pattern. Feynman *et al.* suggested [2] the importance of such a device as a magnetometer [often called superconducting quantum interference grating (SQUIG)], and it was first demonstrated [3] experimentally with six point contacts in 1966. For over 40 years, efforts have focused on the development of equivalent devices with superfluid helium Josephson junctions [4]. Double-path quantum interference pattern was finally observed in superfluid ^{3}He in 2001 (Ref. [5]) and in superfluid ^{4}He in 2006 (Ref. [6]). Here we report the first observation of quantum interference from a ^{4}He grating structure. This multislit matter wave interferometer (consisting of four weak links) is an analogue of the SQUIG. When subjected to an external phase shift, it exhibits the characteristic pattern predicted for four-slit optical interference [7]. The result shows that superfluid ^{4}He interferometers configured as a diffraction grating have the potential to be extraordinarily sensitive phase-shift probes for fundamental physics.

The topology of our superfluid ^{4}He quantum interference grating (SHeQUIG) is shown in Fig. 1. The device consists of four weak link junctions placed in parallel in a loop filled with superfluid ^{4}He. Each weak link is a 50×50 array of nominally 90 nm diameter apertures (spaced 3 μm apart) etched in a 60 nm thick silicon nitride membrane. When a chemical potential difference $\Delta\mu$ is applied across them, the superfluid within these arrays oscillates [8] at the Josephson frequency ($f_J = \Delta\mu/h$). Using a combination of electrostatic force applied to the metallized flexible diaphragm (D) with respect to the fixed electrode (E) and power applied to a heater (not shown) just above the diaphragm, we create and control chemical potential differences. We maintain the mass current oscillation frequency f_J constant (~425 Hz) by a feedback technique. The diaphragm serves as the input element of a sensitive displacement sensor [9], which detects the oscillations. The entire apparatus is immersed in a superfluid helium bath whose temperature is regulated with a stability of ~50 nK. For a general review of superfluid gyrometers, see Ref. [10].

The topmost tube contains a heater (H) at one end and a thin roughened copper sheet (S) at the other that serves as a heat sink to the surrounding helium bath. The heater injects a heat current into the top arm, producing a superfluid counterflow [11], which corresponds to a quantum phase gradient along the tube. Each weak link probes the local phase at four different locations along the top arm. The distance between adjacent phase probes is $d \approx 1.27$ cm, and the cross-sectional area of the heat current tube is $\sigma \approx 3.78 \times 10^{-2}$ cm^2.

Using the two-fluid description [11], the phase difference between two adjacent probing locations (when power $\dot{Q}$ is applied to the heater) can be written as

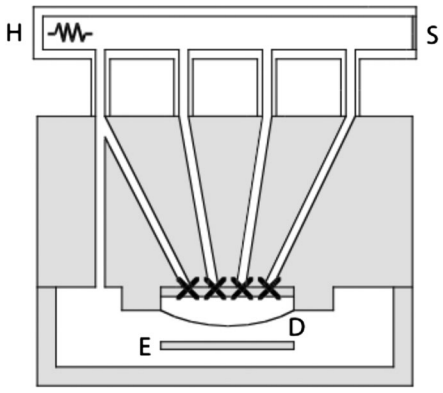

FIG. 1. Experimental apparatus. Crosses indicate the weak link junctions. The inside is filled with superfluid ^{4}He and the entire apparatus is immersed in a bath of liquid helium. A resistive heater (H) and a thin Cu sheet (S) serve as a heat source and sink, respectively. Flexible diaphragm (D) and electrode (E) form an electrostatic pressure pump. The diaphragm also forms the input element of a sensitive microphone based on superconducting electronics that are not shown.

$$\Delta\phi = \frac{m_4}{\hbar}\frac{\rho_n d}{\rho\rho_s T s\sigma}\dot{Q}, \tag{1}$$

where m_4 is the ^{4}He atomic mass, ρ, ρ_n, and ρ_s are the total, normal, and superfluid densities, respectively, s is the entropy per unit mass, and T is the temperature. If N identical weak links (each with current amplitude I_0) are used in the grating, the system should behave like a single junction with critical current amplitude that modulates as [12,13]

$$I_0\left|\frac{\sin(N\Delta\phi/2)}{\sin(\Delta\phi/2)}\right|. \tag{2}$$

Numerical analysis of Eq. (2) shows that the slope at the steepest part of the interference pattern ($|dI/d\Delta\phi|_{(\max)}$) from a grating structure increases as [13]

$$\frac{|dI/d\Delta\phi|_{\text{grating(max)}}}{|dI/d\Delta\phi|_{\text{2-path(max)}}} \approx 0.2N^2, \qquad (N > 2), \tag{3}$$

where $|dI/d\Delta\phi|_{\text{2-path(max)}}$ is the maximum slope for the double-path interferometer. For example, a grating structure with 10 weak links should give a phase change sensitivity 20 times greater than that of a double-path interferometer. If the weak links used are not identical with different oscillation amplitudes $I_0, I_1, I_2, \ldots, I_{N-1}$, the total mass current oscillation amplitude can be written [14] as $(A[0] + 2\sum_{k=1}^{N-1} A[k]\cos(k\Delta\phi))^{1/2}$ where $A[k] \equiv \sum_{q=0}^{N-1-k} I_q I_{q+k}$.

Another practical advantage of using a grating structure (besides the N^2 sensitivity enhancement) has to do with the effect of variations among weak link junctions used in the interferometer. Because of the limitations of nanofabrication technology, all the junctions cannot be made identical. However, in a grating configuration the modulation depth is affected less by nonuniformities compared to a conventional double-path setup. For example, in the extreme case where one of the junctions has zero critical current, a grating structure will still exhibit deep modulation and can be used as a sensitive interferometer. In contrast, a double-path interferometer would show no modulation, giving zero sensitivity.

Figure 2 is an example of experimental data (at fixed temperature) of mass current oscillation amplitude as a function of $\Delta\phi$. [Equation (1) is used to turn $\dot{Q}$ into $\Delta\phi$.] The solid line is a fit using the general function for unequal critical currents with $N = 4$. The striking similarity to a four-slit optical interference pattern [7] can be seen.

The slope at the steepest part of the interference pattern for this grating is ~4.3 times larger than that of a previous superfluid ^{4}He double-path interferometer operating at the same temperature. This observed increase in sensitivity is ~30% greater than what is expected from Eq. (3). We suggest that the extra enhancement is due to weak link nonuniformities which made modulation of the double-path device shallower than that of a grating, as discussed above.

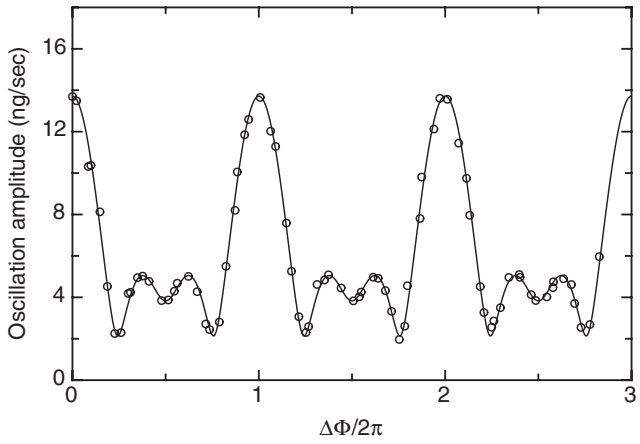

FIG. 2. Measured current oscillation amplitude as a function of $\Delta\phi$ [as given by Eq. (1)]. The solid line is a fit where $I_2 = 0.90I_1$, $I_3 = 1.41I_1$, and $I_4 = 0.46I_1$. These data are taken at $T_\lambda - T \approx 4$ mK. The curve has been shifted horizontally so that the maximum appears at $\Delta\phi = 0$.

The instrumental limit for phase shift measurements for this particular device can be estimated by multiplying $(dI/d\Delta\phi)^{-1}$ by the smallest detectable current $\delta I_{\min} = \rho A\omega_J\delta x_{\min}$ where $A \approx 1$ cm^2 is the diaphragm area, $\omega_J = 2\pi f_J$, and $\delta x_{\min} \approx 3 \times 10^{-15}$ m is the smallest displacement that can be detected in a 1 Hz bandwidth. This gives the smallest detectable phase shift $\delta\phi_{\min} \approx 8 \times 10^{-3}$ rad in a 1 Hz bandwidth if limited by the electronic noise of the displacement sensor. We place our cryostat on a platform supported by three air springs to decouple the experiment from the noisy floor of our building. However, small random rocking motion of the air spring system creates rotationally induced phase noise $\approx 6.2 \times 10^{-2}$ rad/$\sqrt{\text{Hz}}$, which is approximately 1 order of magnitude greater than the electronic background. If the instrument were anchored rigidly in a quieter environment (or if the device were configured as an astatic loop, which is insensitive to rotation), a superfluid interferometer with more weak links configured as in a diffraction grating should become an extremely important scientific probe. For example, if one fabricates a grating structure consisting of 20 junctions (with a 300×300 array of apertures in each weak link) and configures it as a gyroscope with a total sense loop area of 200 cm^2, the smallest detectable angular velocity becomes $\approx 7 \times 10^{-11}$ rad $\cdot$ sec$^{-1}/\sqrt{\text{Hz}}$, which surpasses the resolution of the best atom interferometers [15] ($\approx 6 \times 10^{-10}$ rad $\cdot$ sec$^{-1}/\sqrt{\text{Hz}}$) and starts to approach that of UG1 ring laser gyroscope [16] ($\approx 7 \times 10^{-12}$ rad $\cdot$ sec$^{-1}/\sqrt{\text{Hz}}$). One might fabricate such a grating structure on a single chip using e-beam lithography.

The stability of the device is shown in Fig. 3. The interferometer is held at the steepest part of the modulation curve for about 6 h. The measured noise in the current

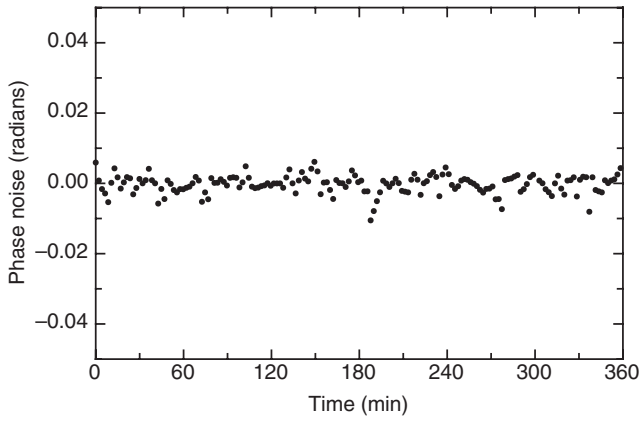

FIG. 3. Phase noise detected over a span of 6 h.

oscillation amplitude has been converted to phase noise using the slope $(dI/d\Delta\phi)$ at the bias point. The measurement has been repeated 5 times, and for all cases, the long-term drift has been found to be $\leq 1.7 \times 10^{-3}$ rad in the 6 h period.

In the case of SQUIGs, the interference pattern becomes more complex due to slight differences in the ''loop'' sizes [13,17]. In the case of a SHeQUIG, as $\Delta\phi$ is increased, the complexity of the interference pattern also starts to increase (see Fig. 4). This arises from the finite widths of the four probes connected to the heat current pipe. (The inner diameter of the 4 tubes is ~0.7 mm at the connection to the heat current pipe and ~2.2 mm everywhere else.) There is a small uncertainty in exactly what location each phase is being read, which makes the exact distances between adjacent probes differ by a finite amount ($\sim \pm$ 0.35 mm). Since the phase difference is $\Delta\phi = d \cdot \nabla\phi \propto d \cdot \dot{Q}$, increasing $\dot{Q}$ (and therefore increasing $\Delta\phi$) results in larger deviations in phase caused by finite deviations in d. This causes the interference pattern to become more complex for large $\Delta\phi$. Thus, there is a trade off in dynamic range when one makes a grating structure rather than a simple double-path configuration.

A SHeQUIG may be of greatest utility for applications where the phase shift of interest is of the order of or less than 2π (or one flux quantum). One such example is the phase shift caused by rotation (Sagnac effect [18,19]). We can envision an interferometer like that shown in Fig. 5. Multiple weak links are connected to a torus with a partition in it. The torus, the inner circular volume, and the pipes connecting the two (through N weak links) are all filled with superfluid ^{4}He. A diaphragm can be placed at the center to detect Josephson mass current oscillations from multiple junctions. With the partition, superfluid in the torus is forced to approximate solid body motion with the rotating Earth. This flow creates a Sagnac phase shift along the torus. As in the experiment reported here, weak links configured as a grating will probe the induced phase at different locations in the torus, and the critical current

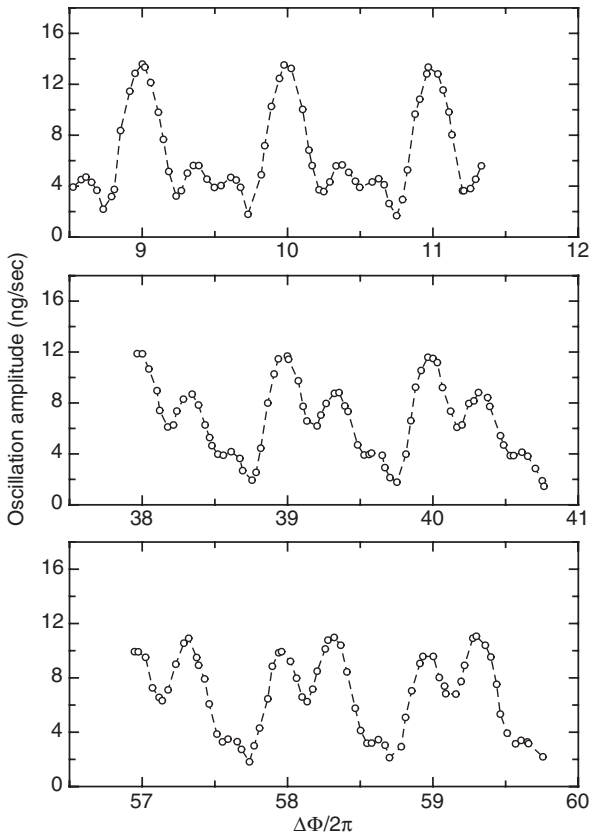

FIG. 4. Interference patterns for large $\Delta\phi$.

will exhibit an interference pattern with diffractionlike sharp peaks. The interferometer configured this way will be an extremely sensitive rotation sensor (i.e., a gyroscope) as mentioned earlier.

There are also small phase shifts expected from novel interactions that have never been probed due to the lack of appropriate sensors. For example, it has been predicted [20] that, in the presence of combined radial electric field and axial magnetic field, superfluid ^{4}He in a torus will have a persistent current in its ground state. (The predicted magnitude [20] for the phase shift accompanying this persistent current is $\approx$0.15 rad if electric field of $\approx 10^7$ V/m and magnetic field of $\approx$1 T are applied to a torus whose radius is $\approx$1 cm.) If the partition is taken out of the torus, the apparatus depicted in Fig. 5 will be an ideal tool to investigate the existence of such phenomenon.

We point out that double-path interferometers are differential sensors for phase shift $\Delta\phi$. When the devices are turned on, there can already be some external phase shift as well as phase bias from vortices trapped in the interferometer loop. This initial phase offset, $\Delta\phi_0$, is practically indistinguishable from $\Delta\phi_0 \pm 2\pi n$ since the double-path interference pattern is 2π periodic in $\Delta\phi$. In contrast, in a multislit grating configuration, the interference pattern evolves as $\Delta\phi$ is increased (Fig. 4) enabling us to distinguish $\Delta\phi_0$ from $\Delta\phi_0 \pm 2\pi n$. In other words, we now have

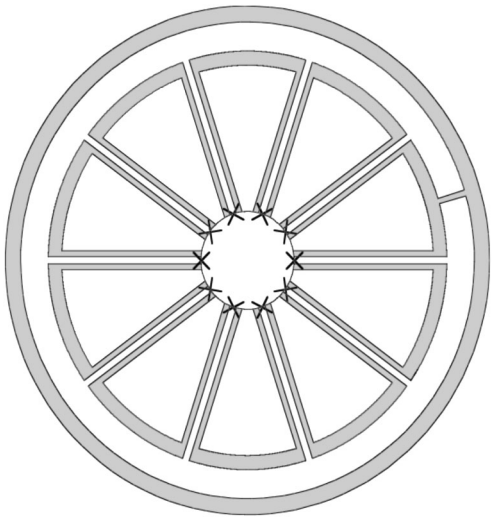

FIG. 5. Possible experimental geometry for a superfluid grating to study Sagnac phase shifts. Crosses indicate weak links. A diaphragm can be placed at the center to detect mass current oscillations. The outer can and a return path needed for the experiment are not shown for the clarity of the schematic.

an absolute gauge (rather than a differential one) that measures quantum mechanical phase differences between any two locations in quantum coherent neutral matter. This sensitivity to absolute phase difference is a by-product of asymmetry in phase probing locations (within the grating) described earlier, and it makes this reported device a different class of interferometer compared with the double-path devices demonstrated in the past. More work is needed to introduce asymmetry in such a way that the device's sensitivity to absolute phase difference can be optimized for future experiments.

In summary, we have demonstrated the first superfluid ^{4}He quantum interference grating which is the analogue of a SQUIG. The interferometer exhibits dynamic behavior similar to that of a single Josephson junction, and the critical current modulates when an external phase shift is introduced in the system. We find that a grating structure can be implemented successfully in a superfluid matter wave interferometer to enhance its sensitivity (to both relative and absolute quantum mechanical phase differences) while trading away some of its dynamic range. The experiment described in this Letter reveals the robust nature of superfluid phase coherence and further advances the close analogy between the macroscopic quantum physics of superconductivity and superfluidity.

Compared to superconducting systems, superfluid quantum interference devices are at a very early stage of development with their ultimate sensitivity and utility still unknown. This reported demonstration of the first superfluid weak link grating should open the door for the development of even more sensitive matter wave interferometers to probe aspects of fundamental physics that have heretofore remained elusive.

We thank Emile Hoskinson for discovering the quantum whistle in superfluid ^{4}He and developing early versions of the lab software and/or instrumentation. We thank Thomas Yuzvinsky for discussions and help with scanning electron microscopy. Inseob Hahn generously provided the high resolution thermometer. This work was supported by the ONR (N00014-06-1-1183) and by the NSF (DMR 0244882). The aperture arrays were fabricated at the Cornell NanoScale Facility, a member of the NSF National Nanotechnology Infrastructure Network.

[1] J. Clarke and A. I. Braginski, *The SQUID Handbook: Fundamentals and Technology of SQUIDs and SQUID Systems* (Wiley-VCH, Weinheim, 2004), Vol. 1.
[2] R. P. Feynman, R. B. Leighton, and M. Sands, *The Feynman Lectures on Physics* (Addison-Wesley, New York, 1965), Vol. 3, Chap. 21, pp. 21–18.
[3] J. E. Zimmerman and A. Silver, Phys. Rev. **141**, 367 (1966).
[4] J. C. Davis and R. E. Packard, Rev. Mod. Phys. **74**, 741 (2002).
[5] R. W. Simmonds, A. Marchenkov, E. Hoskinson, J. C. Davis, and R. E. Packard, Nature (London) **412**, 55 (2001).
[6] E. Hoskinson, Y. Sato, and R. E. Packard, Phys. Rev. B **74**, 100509(R) (2006).
[7] A. Hudson and R. Nelson, *University Physics* (Saunders College Publishing, Philadelphia, 1990), 2nd ed., p. 888.
[8] E. Hoskinson, R. E. Packard, and T. M. Haard, Nature (London) **433**, 376 (2005).
[9] H. J. Paik, J. Appl. Phys. **47**, 1168 (1976).
[10] O. Avenel, Y. Mukharsky, and E. Varoquaux, J. Low Temp. Phys. **135**, 745 (2004).
[11] D. R. Tilley and J. Tilley, *Superfluidity and Superconductivity* (Institute of Physics, Bristol, 1990), 3rd ed.
[12] A. Th, A. M. De Waele, W. H. Kraan, and R. De Bruyn Ouboter, Physica (Amsterdam) **40**, 302 (1968).
[13] J. T. Jeng, K. H. Huang, C. H. Wu, K. L. Chen, J. C. Chen, and H. C. Yang, IEEE Trans. Appl. Supercond. **17**, 691 (2007).
[14] This expression can be obtained by setting $\sum_0^{N-1} I_k \sin(\omega t + k\Delta\phi) = G\sin(\omega t + \alpha)$, and solving for G.
[15] T. L. Gustavson, A. Landragin, and M. A. Kasevich, Classical Quantum Gravity **17**, 2385 (2000).
[16] K. U. Schreiber *et al.*, J. Geophys. Res. **109**, B06405 (2004).
[17] J. Oppenlander, in *Advances in Solid State Physics*, edited by B. Kramer (Springer, Berlin, 2003), Vol. 43, pp. 731–746.
[18] L. A. Page, Phys. Rev. Lett. **35**, 543 (1975).
[19] S. A. Werner, J. L. Staudenmann, and R. Colella, Phys. Rev. Lett. **42**, 1103 (1979).
[20] H. Wei, R. Han, and X. Wei, Phys. Rev. Lett. **75**, 2071 (1995).